



HAL
open science

Valorization of heat-treated wood after service life through a cascading process for the production of lignocellulosic derivatives

Eduardo Robles, René Herrera, Pedro Luis de Hoyos Martínez, Javier Fernández Rodríguez, Jalel Labidi

► To cite this version:

Eduardo Robles, René Herrera, Pedro Luis de Hoyos Martínez, Javier Fernández Rodríguez, Jalel Labidi. Valorization of heat-treated wood after service life through a cascading process for the production of lignocellulosic derivatives. *Resources, Conservation and Recycling*, 2021, 170, pp.105602. 10.1016/j.resconrec.2021.105602 . hal-03202854

HAL Id: hal-03202854

<https://univ-pau.hal.science/hal-03202854>

Submitted on 24 Apr 2023

HAL is a multi-disciplinary open access archive for the deposit and dissemination of scientific research documents, whether they are published or not. The documents may come from teaching and research institutions in France or abroad, or from public or private research centers.

L'archive ouverte pluridisciplinaire **HAL**, est destinée au dépôt et à la diffusion de documents scientifiques de niveau recherche, publiés ou non, émanant des établissements d'enseignement et de recherche français ou étrangers, des laboratoires publics ou privés.



Distributed under a Creative Commons Attribution - NonCommercial 4.0 International License

1 Valorization of heat-treated wood after service life through a cascading process for the production of
2 lignocellulosic derivatives

3 Eduardo Robles^{a,b}, René Herrera^{a,c}, Pedro L. De Hoyos Martínez^a, Javier Fernández Rodríguez^a, Jalel Labidi^a

4 ^a*Biorefinery Processes Group, Chemical and Environmental Engineering Department, Faculty of*
5 *Engineering Gipuzkoa, University of the Basque Country UPV/EHU, Plaza Europa 1, 20018 Donostia,*
6 *Spain*

7 ^b*University of Pau and the Adour Region, E2S UPPA, CNRS, IPREM-UMR 5254, 371 Rue du Ruisseau,*
8 *40004 Mont de Marsan, France*

9 ^c*Innorennew CoE, Livade 6, 6310 Izola-Isola, Slovenia*

10 Abstract

11
12 The present work proposes a cascading approach to fractionate thermally treated wood after life service and
13 untreated wood and their unweathered counterparts. The fractioning of wood was implemented, focusing on
14 the current trends in environmentally friendly processing and processes with a noteworthy yield and purity.
15 Resulting streams: cellulose, hemicelluloses, and lignin. These fractions were analyzed utilizing spectroscopies
16 (ultraviolet and infrared), chromatography (liquid and gas), thermogravimetry, and x-ray diffraction (thermal
17 treatment and weathering). Results showed no significant difference in yielding or the quality of the extracted
18 celluloses (only a slight increment of the crystallinity after the thermal treatment). Considering the hemicellulose
19 fraction, it was observed a considerable mannose reduction after the thermal treatment ($\approx 37\%$) and weathering
20 ($\approx 27\%$), or the combination of both ($\approx 51\%$). Nevertheless, the most notable changes were observed in the yield
21 and the quality of the obtained lignins with higher yields for untreated wood (Po) and more purity ($>93\%$) for
22 lignin samples obtained during the delignification process (L1). Their structure was also affected by the fraction
23 from which they were extracted, as reflected by the S/G ratio. Moreover, the thermal and weathering treatment
24 improved their thermal properties, as shown by thermogravimetric analysis. In general, the present work proved
25 the feasibility of valorizing thermally treated wood after service life within a biorefinery system to obtain
26 competitive value-added products to optimize resources and extend the utility time of such biomass.

27 **Keywords:** heat-treatment, organosolv lignin, cellulose, wood products, fractionation, cascade approach

28 1. Introduction

29 The use of wood-based products in Europe is projected to increase threefold worldwide between 2010 and 2050
30 (Dammer et al., 2016). In this frame, the inventories of Monterey pine (*Pinus radiata* D. Don) in the Basque
31 Country, where is located this research work, has reported an increase in wood production from 15 million m³ in
32 1976 to more than 27 million m³ in 2017 (Etxabe Villasante, 2018). This fact has awakened considerable interest
33 in using this vital resource in high value-added applications after its modification, such as building applications
34 after its thermal or chemical treatment, elaboration of biomaterials, plywood, fiberboards, among others (Wei et
35 al., 2019). Monterey pine is the species that occupy the most significant area (31 % of the total wooden forest
36 area) and about 85-90 % greater forest productivity in the Basque Country. Basque forests can be considered
37 one of the lands with the highest concentrations of Monterey pine in the northern hemisphere; it should be
38 regarded as an essential asset for the local economy (Cantero, 2014). However, the highly fractioned size of
39 private-owned forestlands, the aging of the local population and the strong regulations to cut down have
40 supposed a challenge to the exploitation of pine by the local owners, which often cut down the trees, then leave
41 them as green timber. In this sense, a proficient value-added application has been installing a kiln by local
42 entrepreneurs, who have developed a thermal modification process marketed as Thermogenik[®]. This method
43 has treated local wood samples for outdoor applications such as roofing, decking, and façades. The performance
44 of thermally modified woods has been deeply studied for several applications, showing outstanding
45 results (Herrera et al., 2018). However, in the frame of demands and projections of the XXI century, the mere
46 upgrading of wood or timber as a material is not enough.

47 The thermal modification of wood is an industrial process that take place at temperatures between 170-220 °C
48 in a reduced oxygen atmosphere (e.g. steam saturated, gas, oil) in order to prevent oxidative combustion of the

49 wood components. The thermally modified wood (TMW) presents better dimensional stability, hydrophobicity,
50 and protection against rot fungi (Jones and Sandberg, 2020). The most notable characteristic of the TMW is its
51 color change to darker tones, and durability, which can considerably improve the wood durability class
52 depending on the type of wood and the treatment conditions. The changes in the wood during thermal
53 modification were studied in last decades and several patents and parent were developed. According to the
54 European Committee for Standardization (European Committee for Standardization, 2008) TMW is wood in
55 which the composition of the cell-wall material and its physical properties have been modified by exposure to a
56 temperature higher than 160 °C with limited access to oxygen. The main changes in the wood matrix are the
57 redistribution of lignin components, the degradation of hemicelluloses caused by deacetylation and the acid
58 catalyzed hydrolysis of the polysaccharide chains, cross-linking and repolymerization reactions with different
59 characteristics depending on the species, atmosphere, and temperature(Herrera-Díaz et al., 2019; Jones and
60 Sandberg, 2020; Li et al., 2017).

61
62 The assessment of the process-related environmental impact of heat treatments has been limited; this can be
63 because they lack chemicals and have encouraged the assumption that heat treatments are intrinsically more
64 eco-friendly. According to Sandberg and Kutnar, TMW materials can mitigate climate change and promote
65 sustainable development by reducing energy intake, solid and volatile emissions, reducing pollution, and
66 ecosystem damage (Sandberg and Kutnar, 2016). Despite the industrial expansion of heat treatments,
67 environmental guidelines are becoming more restrictive, and there is an increase in the sensitivity and
68 awareness of the market to the environmental performance of products and services, preferring those that are
69 eco-friendly.

70
71 At the present stage, it is necessary to consider the environmental performance of the thermally modified
72 products and end-of-life scenarios to create strategies after the end of life of products. In general, to develop an
73 environmental performance of a product is necessary to include recycling, upcycling, the cradle-to-cradle/cradle-
74 to-gate paradigm, and end-of-life disposal options. Several studies on ecological solutions in the process stage
75 are performed, mainly focused on releasing volatile compounds into the atmosphere, including recovery by
76 condensation, purification, and successive filtration processes (Herrera et al., 2016a).

77
78 Additionally, the post-service-life reuse or disposal of any material requires strict handling, even for a bio-based
79 material as wood. For this reason, several European countries have developed facilities for the energetic
80 valorization of bio-based materials after their usage (Bentsen and Felby, 2012). Nevertheless, the life cycle
81 assessment of wood as a material is truncated if energetic valorization is the following step after service life
82 (Campbell-Johnston et al., 2020). Instead, the fractionation of the lignocellulosic macro components that
83 constitute wood: holocellulose and lignin carbohydrate and aromatic fractions could open a frame to increase
84 the value and service of wood after its first use, following the principles requested by the circular economy
85 concept, which are considerably demanding nowadays (Islam et al., 2020). In this sense, the cascading approach
86 is considered the most suitable method for the whole valorization of the different biomass fractions. There are
87 three definitions of cascading processes: cascading-in-time, cascading-in-value, and cascading-in-function.
88 Cascading in function has been described as a process through which different products can be produced
89 simultaneously, maximizing the value of the original biomass, resembling the functionality of a biorefinery
90 (Keegan et al., 2013; Olsson et al., 2016; Sokka et al., 2015).

91
92 The most common process to fractionate the wood-based materials is the one applied for the pulp and paper
93 industry, namely, the Kraft process, followed by an elemental chlorine-free (ECF) sequence to bleach the
94 intermediate pulp. However, more environmentally friendly processes can be designed, such as sulfur-free
95 pulping processes or total chlorine-free bleaching sequences (TCF) (Oliaei et al., 2020; Robles et al., 2018).
96 Concerning the pulping stage, the organosolv delignification process includes a diverse range of organic solvents
97 to fractionate lignocellulosic biomass into rich cellulose pulp, a water-soluble hemicellulose stream, and a
98 concentrated lignin fraction. The organic solvents triggered the solubilization of lignin without altering its
99 chemical structure to a high degree, which has positioned these processes into the most attractive ones to

100 preserve the native structure of lignin during the extraction without undergoing strong recondensation reactions
101 (Pandey and Kim, 2011). The high purity of the obtained lignin by these methods, together with the lack of sulfur
102 in its molecular structure, allows lignin to be employed as a source of aromatic structures to produce high
103 added-value chemicals, which can be used for the production of adhesives, binders, in polymer substitutions or
104 as a phenolic precursor (Zakzeski et al., 2010; Zhao et al., 2017). Besides, the low boiling point of the organic
105 solvents allows the recovery of the solvent to avoid its disposal after the process (Fernández-Rodríguez et al.,
106 2020). Thanks to all these advantages, it is expected that the organosolv methods may awaken more industrial
107 interest in the future for biomass fractionation (da Silva et al., 2019).

108
109 For the bleaching stages, the TCF sequences constitute environmentally friendly alternatives to remove the
110 phenolic chromophores from the remaining lignin fraction in the cellulosic pulp without chlorine compounds due
111 to their adverse environmental effects (Ibarra et al., 2006; Nelson, 1998). When doing a TCF bleaching, removing
112 the metals becomes more critical because hydrogen peroxide is applied early in the sequence at higher charges.
113 The elimination of the metals is improved with the addition of a chelating agent. Ethylenediaminetetracetic acid
114 (EDTA) and diethyleneaminepentacetic acid (DTPA) compounds are the best chelating agents for double-charged
115 metal ions. However, using either DTPA or EDTA in "green pulping and bleaching" is currently discouraged as
116 none of these agents is biodegradable, nor are they efficiently handled, as standard water treatment plants
117 cannot remove these components from water. Therefore, they represent considerable harm to the ecosystems
118 in which those streams are deployed. For this reason, it is recommended to use another metal chelating agent,
119 such as the 2,6-Pyridinedicarboxylic acid (PDA), which has been proved to be an effective chelating agent with
120 similar results to those of EDTA (Pinto et al., 2015).

121
122 In the present work, the cascading of local wood residues after its usage to be transformed into bio-based
123 materials by fractionating the whole structure of the macro-components is approached. The goal is to guarantee
124 the integral valorization of these residues by obtaining building block components capable of being transformed
125 into high-value-added compounds. An environmentally friendly and robust process has been designed using an
126 organic acid pretreatment, a sulfur-free delignification stage, followed by a TCF bleaching sequence. This
127 allowed obtaining cellulosic pulp, hemicelluloses, and lignin as main compounds with innovative green
128 processes.

129 2. Material and methods

130 2.1. Materials

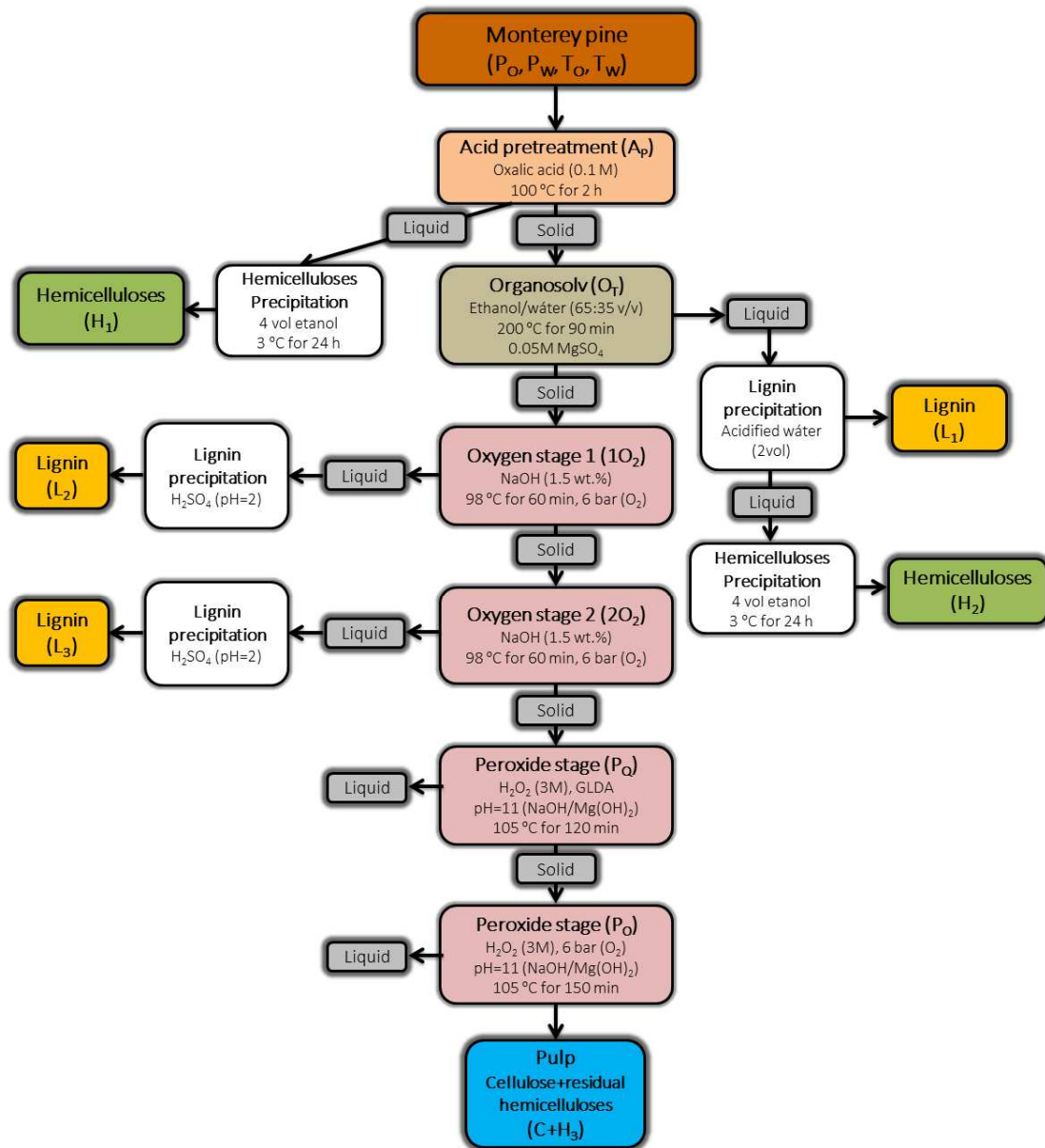
131 Monterey pine (*Pinus radiata* D. Don) was obtained from the forest areas of the Basque Country (Spain). Wood
132 was debarked, sawed, stored, and conditioned before the heat-treatment at Torresar® Company in fulfillment of
133 the chain of custody according to the PEFC certification. The boards of *Pinus radiata* were principally from
134 heartwood with the annular rings at 30 degrees to the face of the board (tangential grain). The load of *Pinus*
135 *radiata* was modified in an industrial chamber according to industrial production standards at 212 °C (Bruno M.
136 Esteves et al., 2020) under a saturated steam atmosphere for 60 h (Termogenik®, Spain). The modification
137 process begins with a rapid increase of the temperature to 100 °C, allowing the drying of the wood to 3–4% of
138 moisture content. Subsequently, steam is sprinkled to avoid wood damage, and the temperature in the chamber
139 is raised to its maximum temperature (212 °C). The last stage is the cooling down and stabilizing of the samples.
140 This stage takes about 24 h, at controlled relative humidity until room temperature to avoid abrupt temperature
141 and pressure fluctuations (Herrera et al., 2016b).

142
143 A set of samples (20 dried wood and 20 thermally modified wood) with the dimensions of 9 x 170 x 170 mm
144 were exposed twelve months to natural weathering in wooden support at 45 degrees of inclination and facing
145 south direction (from May to April) in a location with oceanic climate (San Sebastian, Spain: 43°18'33.054"
146 Latitude N; 2°0'34.817" Length W). Subsequently, weathered samples were conditioned at 20 °C and 65% RH
147 before analysis reported previously (Bruno M. Esteves et al., 2020). Samples of dry Monterey pine (Po),
148 weathered dry pine (Pw), thermally treated pine (To), and weathered thermally treated pine (Tw) were

149 statistically selected to compare the influence of the weathering process on the lignocellulosic components of
150 pine and thermally treated pine. In detail, a multiple comparison procedure analysis of variance (ANOVA) was
151 used to determine which means were significantly different from others, and the confidence levels were
152 examined. Bonferroni Significant Difference (BSD) was applied after rejecting the null hypothesis. The software
153 used for this statistical and graphing analysis was OriginPro 9.7.0.185.

154 2.2. Fractionation processes

155 The stages of the fractioning were selected to develop a globally environmentally friendly process to leverage all
156 the lignocellulosic platforms as different biomaterials from this forestry product after the end-life, as reported by
157 this group (Fernández-Rodríguez et al., 2017b; Robles et al., 2018). For this purpose, acid pretreatment,
158 organosolv treatment, and totally chlorine-free bleaching were selected. These stages constitute a sustainable
159 process, focusing on the low environmental impact of the chemicals used through all the involved steps. All the
160 reactions were carried out in a 4 L Zipperclave (Autoclave Engineers, Division of Snap-tite, Inc.) with PC-
161 controlled stirring, pressure, and temperature. The global flowsheet of the followed process and the description
162 of the obtained samples are detailed in Figure 1.



163
164 Figure 1. Flowsheet of the process and the recovered fractions.

165 2.1.2. Acid pretreatment (A_p)

166 All samples were chipped to an average of 10 mm chips and washed with a 0.1 M oxalic acid solution for 2 h at
167 100 °C (Barana et al., 2016). Hemicelluloses were precipitated from the liquid fraction with 4 volumes of ethanol
168 at 3 °C for 24 h (Reyes et al., 2013), after which the solid precipitate was separated by centrifuging the
169 suspension and washing the pellet until neutral pH was achieved; ethanol used in this stage was recovered via
170 rotary evaporation and used for the following stage. The recovered solid fraction was called H1; an aliquot of the
171 liquid after centrifuging was kept to analyze non-precipitated sugars.

172 2.1.3. Organosolv delignification (O_T)

173 The organosolv process was conducted using a mixture of ethanol/water (65:35 v/v) as a solvent, at 200 °C for
174 90 min and fiber to liquid ratio of 1:10 (w/v), adding 0.05M MgSO₄ as catalyst (Nitsos et al., 2018). The liquid

175 fraction was separated via filtration, and the solid fraction was washed several times until driving the remaining
176 fibers to a neutral pH. Lignin (L₁) was precipitated from the spent liquor by adding two volumes of acidified
177 water (pH = 2), after which the solid fraction was filtered with a 0.22 μm membrane. Hemicelluloses that could
178 be extracted during this process were isolated by the remaining filtrate concentration, adding 4 volumes of
179 ethanol, and kept at 3 °C for 24 h; afterward, the solid precipitate (H₂) was isolated by centrifugation.

180 2.1.4. Bleaching sequence

181 The Totally Chlorine Free Bleaching sequence was designed to purify the fibers obtained during the
182 delignification stage. This sequence was based on two alkaline oxygen stages (1O₂ & 2O₂); one stage hydrogen
183 peroxide with a secondary chelating reaction (P₀) and the final one with alkaline peroxide under oxygen
184 atmosphere (P₀). Oxygen-alkaline stages (1O₂ & 2O₂) were equally carried out with 1.5 wt% NaOH for 60 min at
185 98 °C, and the pressure of the autoclave was maintained at 6 bar using O₂ atmosphere (Ibarra et al., 2006). The
186 liquid waste fractions from these stages were collected to precipitate lignin by their acidification using H₂SO₄ (96
187 wt%) until pH = 2. In this sense, two more lignin fractions were obtained (L₂ and L₃). The first stage with
188 hydrogen peroxide was done using 3M H₂O₂, at pH=11, stabilized with a mixture of NaOH and Mg(OH)₂ (3:1
189 wt%). The use of Mg(OH)₂ as a partial substituent of NaOH was effectuated as it has been reported its efficiency
190 as an alkaline agent for peroxide bleaching with a 30% substitution being the optimal (Kong et al., 2009). The
191 reaction was performed for 120 min at 105 °C with N, N-bis(carboxymethyl)glutamic acid (GLDA, CAS: 58976-65-
192 1) as a chelating agent. GLDA constitutes an environmentally friendly substitution of the traditional chelating
193 agents, such as EDTA or DTPA, which are difficult to be eliminated from water effluents (Koodynska, 2011). The
194 final stage was performed using at 105 °C for 150 min; the reaction was kept under constant pressure of 6 bar of
195 an O₂ atmosphere (Robles et al., 2018). In this stage, a 3M H₂O₂ was used, the pH was stabilized at pH=11 with
196 NaOH, without any chelating agent. For all the reactions, the liquid to solid ratio was 10:1 (w/v).

197 2.2. Analytical methods

198 The initial characterization of the raw material was carried out according to standard methods developed by the
199 Technical Association of the Pulp and Paper Industry (TAPPI): moisture (TAPPI T 264 cm-07, 2007), inorganic
200 content (TAPPI T 211 om-16, 2016), ethanol-toluene extractives (TAPPI T 204 cm-07, 2007) Klason lignin (TAPPI T
201 222 om-11, 2011), holocellulose (Wise et al., 1946), cellulose, and hemicelluloses (Pettersen, 1984) were
202 quantified. Scanning electron microscopy images were obtained with a Scanning electron microscope JEOL JSM-
203 6400 F with field emission cathode and a lateral resolution of 10-11 Å at 20 kV. Samples were analyzed by
204 Fourier Transform Infrared Spectroscopy (FT-IR) with a PerkinElmer Spectrum Two Spectrometer, equipped with
205 a universal Attenuated Total Reflectance (ATR) accessory with an internal reflection diamond lens. The defined
206 range of wavelength was from 4000 to 400 cm⁻¹ and the resolution 4 cm⁻¹. For each sample, 30 scans were
207 recorded.

208
209 The cellulose fraction was analyzed by X-ray diffraction with a Panalytical Phillips X'Pert PRO multipurpose
210 diffractometer. Samples were mounted on a zero background silicon wafer fixed in a generic sample holder,
211 using monochromatic CuKα radiation (λ = 1.5418 Å) in a 2θ range from 5 to 50 with a step size of 0.026 and 80 s
212 per step at room temperature. The NMR spectrometry for ¹³C was performed using a Bruker 500 MHz
213 spectrometer (Billerica, MA, USA) at 250 MHz of frequency at room temperature. The spectrum was recorded
214 with cross-polarization and magic-angle spinning.

215
216 The samples from the stages where the hemicelluloses were precipitated, namely H₁ and H₂, were analyzed via
217 high-performance liquid chromatography (HPLC). This analysis was performed using a Jasco LC Net II/ADC
218 chromatograph equipped with a refractive index detector and a diode array detector to determine the
219 concentration of the main monomeric sugars (glucose, xylose, arabinose, and mannose) and degradation
220 products (acetic acid and formic acid). These compounds were analyzed using a column Phenomenex Rezex
221 ROA. The mobile phase was a solution of 0.005N H₂SO₄ with a flow rate of 0.35 mL min⁻¹ and a column
222 temperature of 40 °C. For this analysis, the solid samples of H₁ and H₂ were previously dissolved in acidified

223 water, and then they were filtered through membranes of 0.22 μm pore size. For the quantification of the main
224 monomeric sugars and degradation products, standards of high purity and a known concentration of D-(+)-
225 glucose, D-(+)-xylose, D-(-)-arabinose, and D-(+)-mannose, acetic acid glacial and formic acid were employed.

226 Lignin was evaluated in terms of purity and composition, measuring the Acid Insoluble Lignin (AIL), as well as
227 Acid Soluble Lignin (ASL) following standard methods for quantifying the purity of sulfur-free lignin samples
228 (TAPPI T 222 om-11, 2011; TAPPI T 249 cm-09, 2009). Carbohydrates extracted during the AIL method were also
229 determined by High-Performance Liquid Chromatography (HPLC), following the same method described above.

230 The molecular weight average (M_w) and polydispersity index ($M_w M_n^{-1}$) were measured by Gel Permeation
231 Chromatography (GPC) using a Jasco LC-Net II/ADC device, equipped with a reflex index detector, PolarGel-M
232 column (300 mm, 7.5 mm), and PolarGel-M guard (50 mm 7.5 mm). Samples were prepared in
233 dimethylformamide with 0.1 % lithium bromide as a mobile phase, injected using a 0.7 mL min^{-1} flow at 40 $^\circ\text{C}$.
234 The calibration was carried out using polystyrene standards ranging from 266 to 70,000 g mol^{-1} .

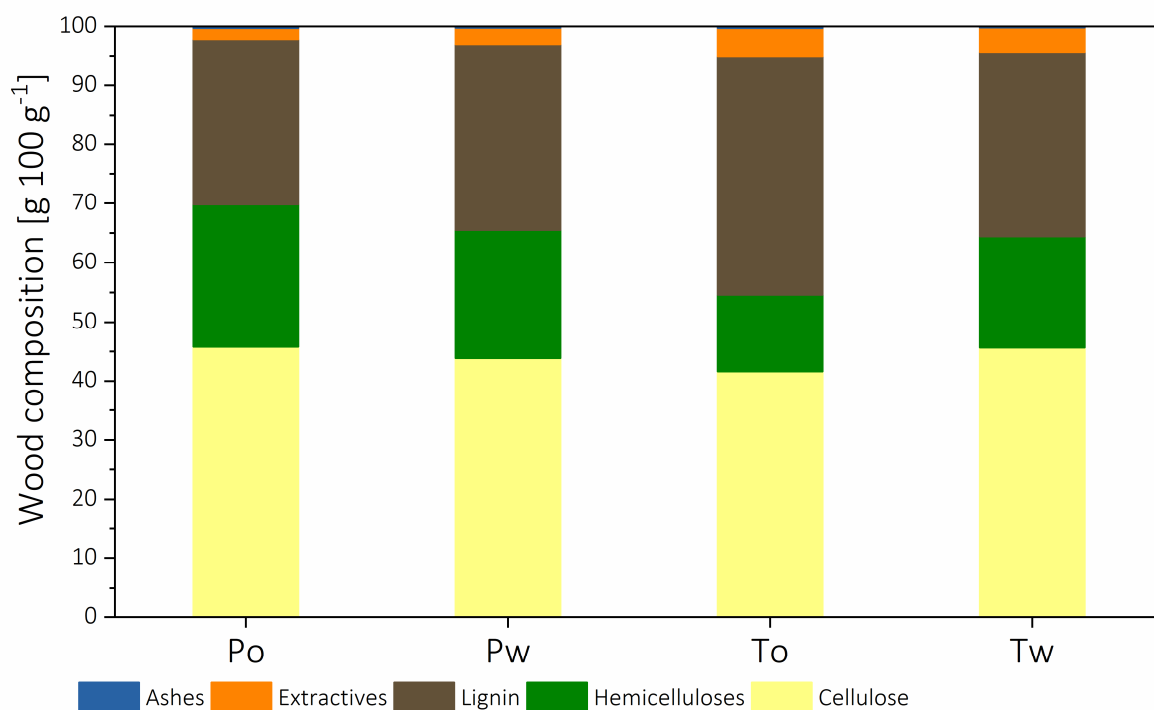
235 In addition, lignin samples were characterized by pyrolysis–gas chromatography–mass spectroscopy (Py–GC–
236 MS), where each sample was thermally degraded in an inert atmosphere, after which its macromolecules break
237 down at specific lower bonding energy points, forming volatile fragments that provide useful structural
238 information about lignin as a whole. The Py–GC–MS was carried out following the method described by this
239 group using a commercial pyrolyzer (Pyroprobe model 5150, CDS Analytical Inc., Oxford, PA) (Herrera et al.,
240 2014). A Thermogravimetric Analysis (TGA) was also carried out to determine the thermal transitions and the
241 thermal stability of the lignins. This characterization was carried out in a TA Q2500 calorimeter, with a 10 $^\circ\text{C min}^{-1}$
242 heating ramp, from 30 to 800 $^\circ\text{C}$ under an N_2 atmosphere.

243 3.1. Results and discussion

244 3.1 Feedstock characterization

245 As the first step, it is shown in Figure 2 the characterization of the different feedstock used in this work. As it can
246 be seen, during the weathering of the non-thermally treated material (Pw vs. Po), the percentages of the
247 carbohydrate macrocomponents (celluloses and hemicelluloses) were reduced, whereas the portion of lignin
248 increased, showing in all cases a significant difference at the $p < 0.05$ level. This involves the weathering affected
249 mainly the polysaccharides that are easier to be degraded (hemicelluloses and the amorphous cellulose section).
250 On the contrary, it was more difficult to degrade the aromatic lignin structures, which led to an increase in the
251 lignin percentage in Pw. The use of the thermally treated sample (To vs. Po) provoked the same effect as the
252 weathering, but more intense, with a higher decrease of the percentage of carbohydrates (especially
253 hemicellulose, which showed a significant reduction at the $p < 0.05$ level) and the corresponding increase of the
254 lignin fraction. This was caused by the solubilization of the hemicelluloses and the small amorphous portion of
255 the cellulose, remaining the lignin in a bigger concentration due to its stabilization by the polycondensation
256 reactions of lignin undergone during the thermal treatment, as reported by Herrera and collaborators (Herrera
257 et al., 2016a). However, a trend change was experienced when the weathering was applied over a thermally
258 treated material (To) since the carbohydrate platform increased in percentage of the remaining material after
259 the weathering. At the same time, the lignin content was decreased, in the opposite tendency as in Pw. The
260 reason is based on the influence of the thermal pretreatment, as during this step, the carbohydrate composition
261 that was more prone to be extracted was already solubilized, this resulted in no significant differences ($p < 0.05$)
262 between the lignin content of Pw and Tw. In this sense, the portion of carbohydrates still in the feedstock was
263 more recalcitrant to be degraded by the exposure to the environment. Therefore, the removal of some
264 carbohydrates during the thermal pretreatment led to generating a substrate more resistance and steady during
265 the weathering exposure, as the weaker parts of the carbohydrate platform were already extracted, which can
266 be considered a strong advantage of the thermal treatment. Nevertheless, the lignin composition increase led to
267 higher availability, comparing To against Po, to be attacked by the weather conditions, since lignin is a sensitive
268 component to be photo-degraded by weathering (George et al., 2005).

269



270
271

272 **Figure 2.** Chemical composition of the used biomass (Po: Monterey pine; Pw: weathered pine; To: treated pine;
273 Tw: weathered thermally treated pine), further information is presented in Table S7.

274

275 3.2. Fractionation yields

276 The relative extraction yields for each recovered fraction (cellulose, lignin, and hemicelluloses) were presented
277 in Figure 3. Tables S1 to S6 present additional information concerning the recovered fractions after each
278 process.

279 The extraction yield of cellulose (C1), expressed as the cellulose content of the pulp obtained after the whole
280 process, showed similar yields for the materials that were not thermally treated (Po and Pw). However, there
281 was a decrease in the cellulose yield in the case of To (45.46%). Therefore, the thermal treatment provoked a
282 decrease in cellulose in the initial material, as shown in Figure 2. This different behavior of To was not
283 experienced by Tw, as the extraction yield (61.11%) was closer to the Ry of Po (65.9%) and Pw (64.07%). Thus, in
284 this case, the weathering mitigated the influence of the thermal treatment.

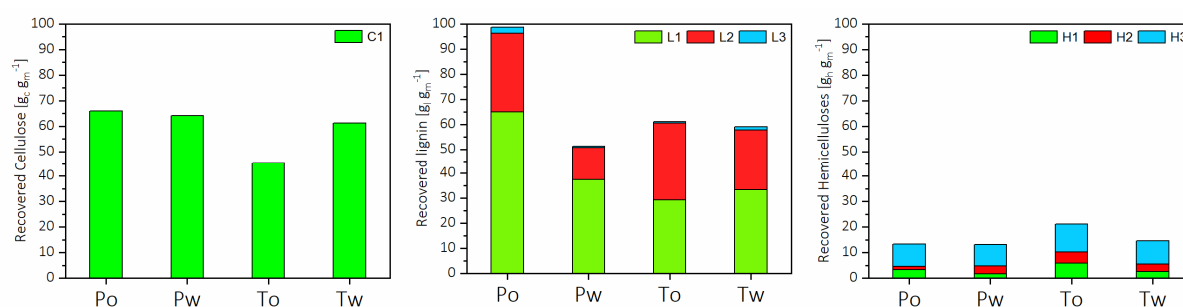
285 From the lignin yields, it can be established that the process to extract lignin by this route was adequately
286 designed as it allowed almost a total Ry for the Po, with a total lignin extraction (L1+L2+L3) of around 98.62%.
287 However, when the initial material was subjected to thermal treatment or a weathering period, the extraction of
288 lignin in the O_T stage was deeply impacted, with a reduction of L1 from ≈65% in Po to 30-40% for the other
289 feedstock. Regarding the yields from different stages, the main extraction occurred during the organosolv
290 process (L1) as was expected, especially in non-thermally treated pine (Po and Pw). Although the L1 samples
291 from the thermo-treated wood (To and Tw) showed lower extraction yields for L1, the yields for L2 (31.15% and
292 24.33%, respectively) were similar to L2 extraction yields for Po and Pw (31.35% and 13.18%). The reason can be
293 based on the new nature of the remaining lignin or para-lignin after the thermal treatment, as reported before
294 (Herrera et al., 2014), where it was pointed out that the original lignin undergoes several reactions of
295 polycondensation above 190 °C. These reactions are caused by the initial demethoxylation of the methoxy
296 groups of guaiacyl and syringyl units that allowed free ortho sites in the aromatic rings to be cross-linked with
297 other components fragments of cellulose and hemicelluloses when the temperature was above 190 °C. This
298 more condensed structure is less sensitive to be extracted by the solubilisation with organic solvents (O_T),
299 whereas it is possible to be degraded and extracted by the alkaline treatment applied during the 1O₂ and 2O₂
300 stages. Therefore, it was justified the inclusion of the lignin precipitation stage after the 1O₁ stage. On the

301 contrary, the fraction of L3 recovered after the 2O₂ stage was inefficient, based on the low extraction yields (0.5-
302 2.5% for all the materials). Thus, this fraction could be considered almost negligible.

303 Hemicelluloses recovery resulted in low yields regardless of the feedstock. This is caused because for
304 hemicelluloses (H1, H2, and H3), only solid fractions were considered, not the small fractions (sugars and acids)
305 that were not capable of being precipitated by the method described before. In any case, the extraction stages
306 (A_P y O_T) were intentionally designed using mild conditions to allow the extraction of the hemicelluloses without
307 degrading them into their monomeric compounds. H1 and H2 were the precipitated fractions from A_P and O_T,
308 whereas the H3 was comprised in the solid fraction in the final recovered pulp after the bleaching sequence. This
309 is why H3 obtained a higher recovery yield since only the bigger molecular compounds of the extracted
310 hemicelluloses could be isolated by this precipitation method. While this technique could not recover the
311 monomeric sugars and small oligomers, which were neglected due to the low concentration, it was quantified in
312 the liquid streams and their difficulty to be valorized in value-added applications. This is due to their lack of
313 biocompatibility based on the pH of the extracted liquid streams, despite the approach followed in other works
314 (Gullón et al., 2020). Consequently, the most remarkable yield was reached by To, because the remaining
315 hemicelluloses after the thermal treatment are more condensed and more accessible to be isolated by their
316 precipitation, despite their lower composition in the feedstock.

317 Regarding process efficiencies (the total amount of solids recovered after fractionation), they were similar during
318 the first two processes: the process efficiency of Organosolv 84.18% and the first alkaline extraction 85.19 %
319 (tables S2 and S4 respectively of supporting information). During the second alkaline extraction, the efficiency
320 was almost 100%, while the recovered lignin was, in every case, less than 1 g_l g_m⁻¹; the recovered solid fraction
321 was practically not changed. This can be related to the process reaching its inherent feasibility to extract lignin, a
322 phenomenon observed in previous work from De Hoyos-Martínez and collaborators (de Hoyos-Martínez et al.,
323 2018), and less pronouncedly in the work of Fernández-Rodríguez and collaborators (Fernández-Rodríguez et al.,
324 2017b), in which sequential treatments of similar nature resulted in considerably lower yields. Process
325 efficiencies of hydrogen peroxide stages (P) correspond to the recovered bleached pulp, as no other product
326 could be recovered; in the case of the first stage (P₀), the mean process efficiency was 75.51%, being 83% for
327 pinewood and 72% for thermowood. It can be appreciated that the total lignin recovered corresponded to a
328 total of 98.63 % for P₀ and 61.00% for T₀ without weathering, while the recovery of lignin after weathering was
329 51.19% for P_w and 58.94% for T_w. This implies that the lignin recalcitrance for extraction with the Organosolv
330 and 1O₂ bleaching stage does not change after weathering for T samples, while for P, it has an important
331 decrease in the effectiveness during the 1O₂ stage.

332

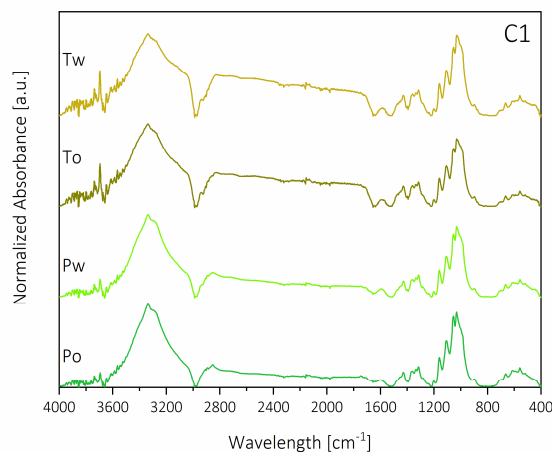


333
334 **Figure 3.** Yields of each recovered solid fraction concerning the initial macrocomponent amount reported in
335 Figure 2. C1 is the cellulose content of the bleached pulp. L1 is the organosolv lignin, L2 is the alkaline lignin from
336 bleaching sequence O1, L3 is the lignin from bleaching sequence O2. H1 is the hemicelluloses from acid
337 pretreatment, H2 are the hemicelluloses from organosolv, and H3 are hemicelluloses remaining in the bleached
338 pulp.

339 3.3. Physico-chemical characterization of the obtained products

340 3.3.1. Cellulose fraction

341 Infrared spectrometry analysis was performed on the cellulose fractions recovered to evaluate their structure
342 (Figure 4). Infrared spectra of bleached pulp (C1) show a broad band at $3600\text{--}3000\text{ cm}^{-1}$, attributed to free
343 vibrating hydroxyl groups characteristic of cellulose. Bands corresponding to $\nu(\text{C-H})$ and $\nu(\text{CH}_2)$ locate between
344 $3000\text{--}2800\text{ cm}^{-1}$ displayed a weak intensity before thermal treatment of wood; in the case of To and Tw, they
345 are almost imperceptible. Regarding the fingerprint region, it can be identified a band at 1430 cm^{-1} related to
346 Methyl-O-CH₃ bonds and a band at 1370 cm^{-1} corresponding to C-H bond in $-\text{O}(\text{C}=\text{O})\text{CH}_2$ group. Bands at
347 1317 and 1200 cm^{-1} are attributed to -OH groups in-plane bending, while the band at 1160 cm^{-1} corresponds to
348 the C-O-C anti-symmetric bridge stretching in cellulose. Below 1200 cm^{-1} , there can be identified two bands at
349 1100 and 1055 cm^{-1} corresponding to C-OH and C-O stretching, and finally, a band at 900 cm^{-1} that corresponds
350 to the β -glucosidic linkages between sugar units (Kruer-Zerhusen et al., 2018). In this fingerprint region, there is
351 no particular difference between the analyzed celluloses, which implies that the chemical structure of cellulose
352 is not significantly affected by either the thermal treatment or the effects of weathering.
353

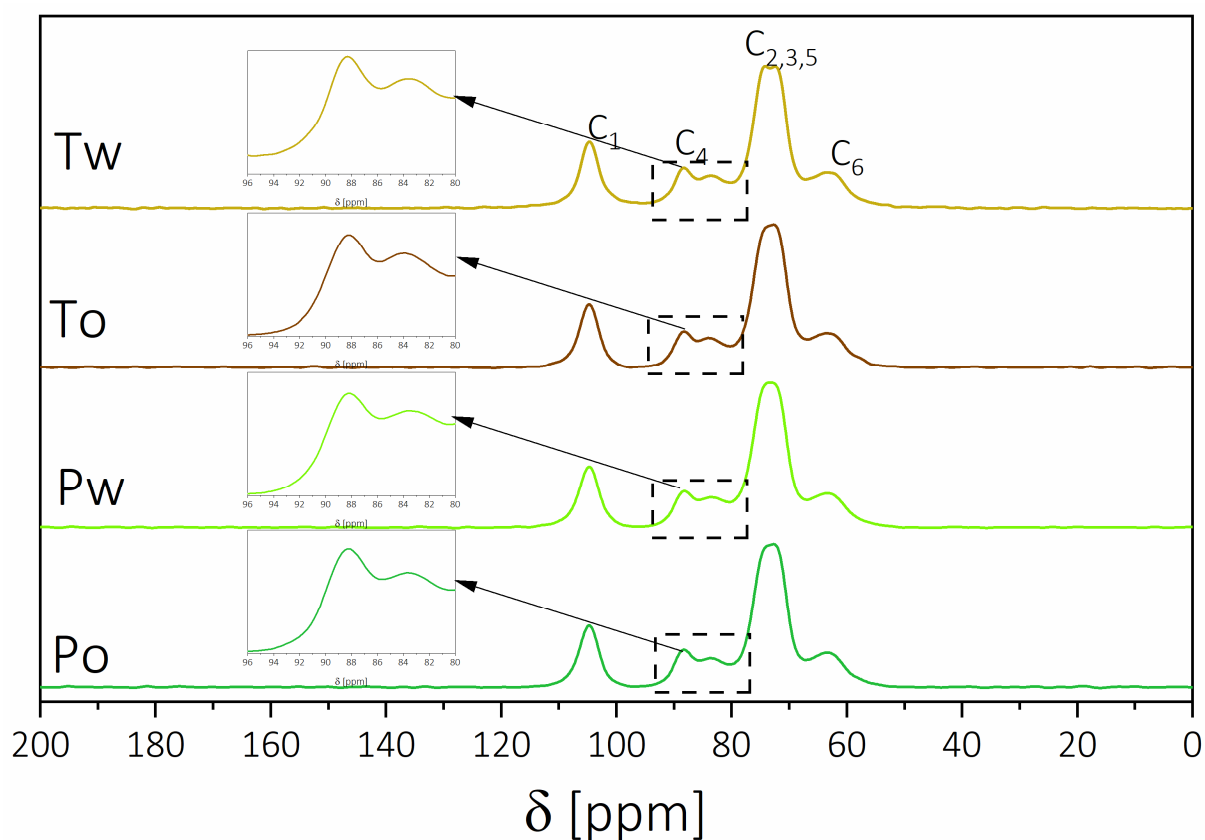


354
355

Figure 4. Infrared absorbance spectrograms of the obtained celluloses.

356
357
358
359
360
361
362
363
364
365
366
367
368
369
370

Figure 5 presents the ^{13}C CP-MAS NMR analysis of the obtained bleached pulps, composed mainly of cellulose. Insets present a magnification of the C4 region, which is considered a referent to identify the more ordered structures of cellulose I. NMR analysis shows that the structure of pulps was practically invariable despite weathering. This consistency was a positive outcome if weathered thermally treated wood would be considered as raw material for the pulp and paper industry during a cascading use of such material. The main difference observed was between Po and Pw, with an increase of the amorphous region of the C4 chemical shift, while for To and Tw, the change in proportions was inverse, with Tw having a sharper shift at the ordered region (92-86 ppm). This change can be related to the transformation of low molecular carbohydrates during treatment, which reacted with lignin and leached during weathering. This resulted in a pulp enriched in more crystalline and ordered cellulose, which is a phenomenon already reported to happen in thermally treated wood regardless its origin (softwood or hardwood), previous authors have reported maximal crystallinity being reached around 210 °C, similar to the conditions used in this work (Durmaz et al., n.d.; Yildiz and Gümüşkaya, 2007).

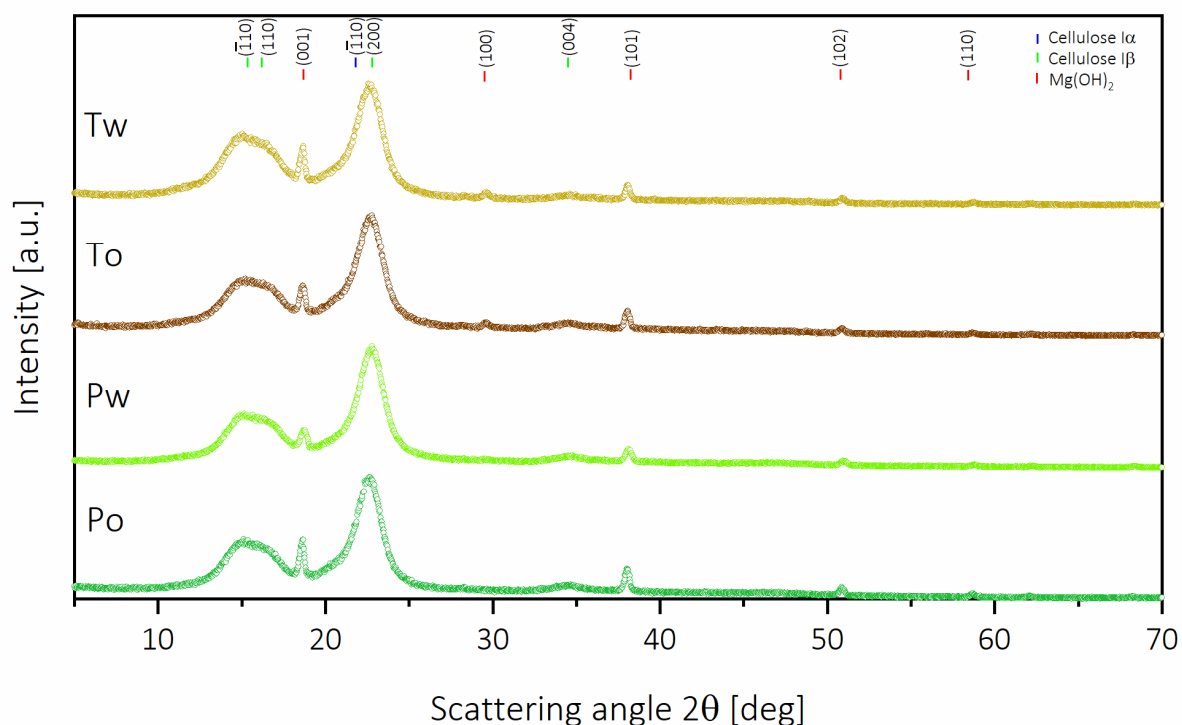


371
372
373
374
375
376
377
378
379
380
381
382

Figure 5. NMR spectra of the obtained celluloses

The x-ray diffraction patterns of the bleached pulps are presented in Figure 6. Three main components can be observed, cellulose I β , which was the major component, as it is typical for native celluloses, cellulose I α in a minor proportion, and traces from Mg(OH) $_2$, which were residuals from the first alkaline-oxygen bleaching stage. As calculated from the XRD patterns with the peak fitting method and subtracting the contribution made by Mg(OH) $_2$, crystallinities were in general high, with Po having 70.4%, Pw 68.25%, To 73.69, and Tw 71.48%. This means that crystallinity was slightly increased during thermal treatment, mainly due to interaction between amorphous cellulose with lignins to form lignin-carbohydrates complexes (LCC), but it was also reduced after weathering because of cellulose degradation. It can be concluded that there was a direct relationship between the crystallinity of the cellulose and its affinity to keep Mg(OH) $_2$ attached to the pulp when comparing results

383 from Figures 5 and 6. Po and Tw were the ones having more intense signals corresponding to the Mg(OH)₂
 384 (Maskal and Thompson, 1971; Ni and He, 2004).



385
 386 **Figure 6.** X-ray diffraction patterns of the different celluloses.

387 **3.3.2. Hemicellulose fraction**

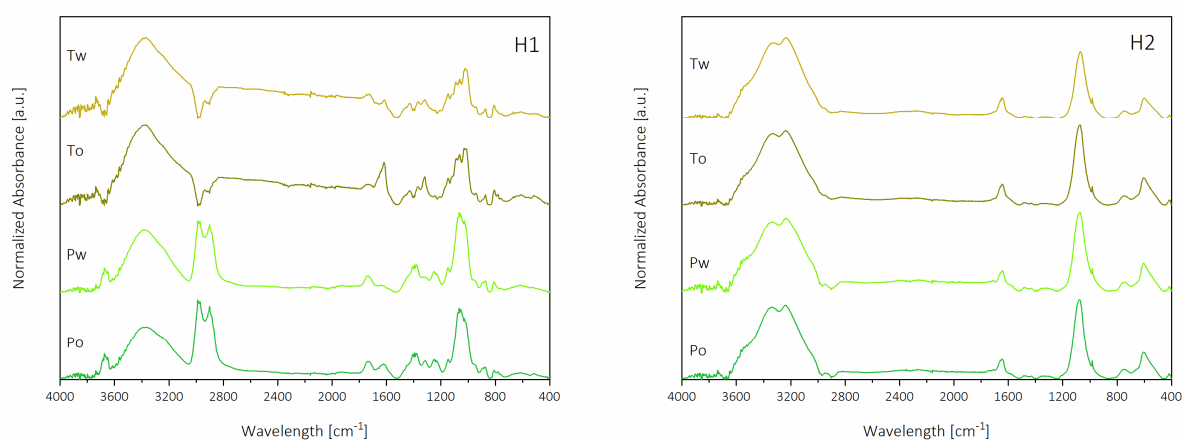
388 Pure hemicelluloses streams were recovered from two different stages of the global process; leaching (H1) and
 389 organosolv (H2), as H3 was contained within the final pulp stream. Their monomeric composition characterized
 390 these precipitates both in sugars and in acids, whose quantified amounts are presented in Table 1. The most
 391 common sugar was mannose-related oligosaccharides, as expected from softwood (Santos et al., 2018). The
 392 presence of mannose in H1 was affected by two parameters. First, the thermal treatment, showing a decrease of
 393 ≈37% in To compared to Po, and the second was the weathering, having Pw a decrease of ≈23% compared to Po.
 394 When both parameters were present (Tw), the decrease in mannose concentration was ≈51%. This means that,
 395 while the cellulose was preserved almost identical through the treatment and weathering, the oligosaccharides
 396 present in the pinewood were more severely affected by these two parameters, with xylose concentrations and
 397 arabinose oligosaccharides suffering similar tendencies in the case of H1. On the other hand, H2 samples were
 398 more similar; however, the overall purity was strongly diminished; this is due to the severity of the treatment,
 399 but also because of the difficulty to recover dissolved polysaccharides from organosolv liquors, given the fact
 400 that hemicelluloses precipitate in organic solvents (Peng et al., 2012).

401
 402 **Table 1.** The concentration of monomeric sugars and acids in the recovered products (expressed in mg L⁻¹).

	H1				H2			
	Po	Pw	To	Tw	Po	Pw	To	Tw
Xylose	5.21	2.32	1.11	2.19	0.13	0.45	1.34	2.36
Arabinose	3.99	2.71	1.15	2.22	1.81	0.58	2.20	2.83
Acetic acid	3.03	2.47	9.71	3.52	6.41	2.00	2.84	10.47
Formic acid	-	-	3.34	-	-	1.99	-	-
Mannose	45.31	34.75	28.38	22.07	14.84	12.95	13.63	12.72

403
 404 The infrared spectra of hemicelluloses obtained from the acid leaching (H1) presented a broad band at 3600-
 405 3000 cm⁻¹ corresponding to hydroxyl groups stretching of the mannose and xylose units in hemicellulose

406 molecules. A band at 2000-2700 cm^{-1} corresponded to -CH bond deformation of -CH₂ and -CH₃, these bands
 407 were absent in To and Tw, meaning that most of the hemicelluloses were depolymerized during the
 408 hydrothermal treatment (Boonstra and Tjeerdsma, 2006). The spectra of H1 from To and Tw were more similar
 409 to xylose, showing weaker bands attributed to C-H vibrations of mannose (1500-1200 cm^{-1}) than Po and Pw, and
 410 weak peaks associated with xylose (1200-900 cm^{-1}), thus showing xylose degradation (Wang et al., 2013).
 411 Hemicelluloses obtained from the Organosolv treatment (H2) presented fewer differences between each other.
 412 Thus, increasing the severity of the treatment, the obtained samples were more homogeneous regardless of the
 413 used feedstock in the process. In H₂, it can be highlighted the identifiable bands corresponding to hydroxyl
 414 groups (3600-3200 cm^{-1}), the band at 1650 cm^{-1} corresponds to CO stretching of carboxylate in either salt or
 415 ester form (Z. Chen et al., 2015). Finally, characteristic C-O-C stretching of the pyranoid ring of xylan was
 416 observed at 1060 cm^{-1} , and the band corresponding to β -glucosidic linkages between xylose units is present at
 417 890 cm^{-1} (Sun et al., 2013). Results from infrared spectra were concurrent with the concentration analysis,
 418 showing a reduction in mannose concentration for H1 in To and Tw compared with Po and Pw; while for H₂, the
 419 spectra presented lower variations.
 420



421
 422 **Figure 7.** Infrared absorbance spectrograms of the obtained hemicelluloses from acid pretreatment (H1) and
 423 organosolv (H2).

424 3.3.2. Lignin fraction

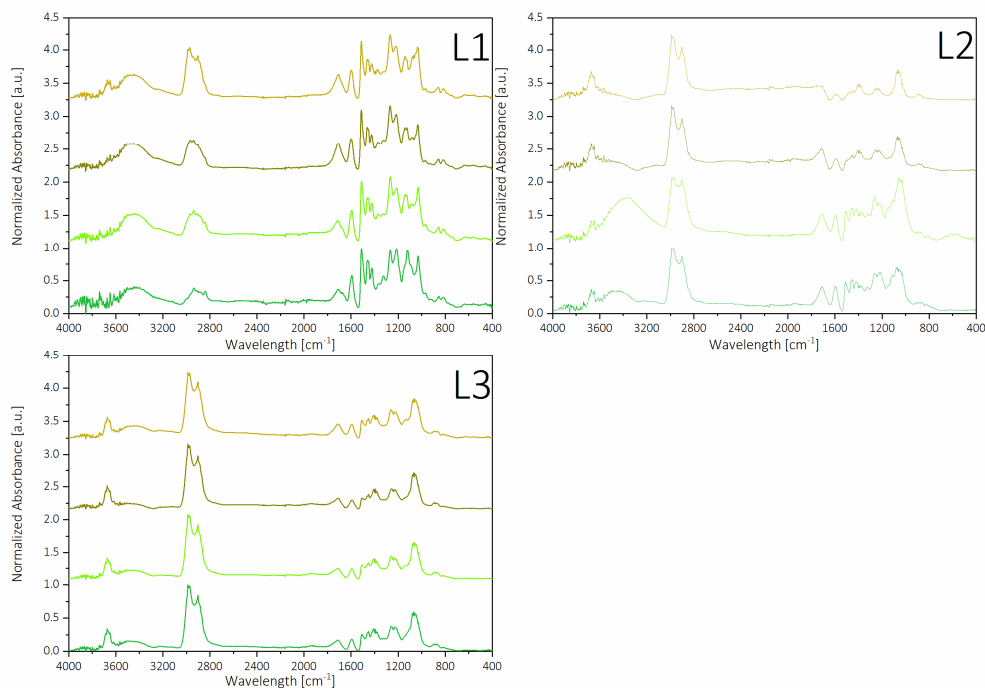
425 Table 2 presents values corresponding to acid-insoluble lignin (AIL), acid-soluble lignin (ASL), residual
 426 carbohydrate contents, ashes, molecular weight (Mw), and polydispersity index (M_w/M_n) of the obtained lignin
 427 samples. The aggregate of ASL and AIL is related to the purity of the obtained lignin, in which it can be observed
 428 a high purity of the organosolv lignins (L1) with no significant differences between the samples extracted from
 429 the different feedstock (93-95% for all of them). This means that despite the differences between yields, the
 430 properties of lignins obtained by the O_T stage shared the same composition. Besides, the higher purity of the
 431 isolated lignin, compared to other results presented in the literature (Hosseinaei et al., 2016; Toledano et al.,
 432 2013), could be based on introducing the pretreatment stage, where the carbohydrate compounds that could
 433 pollute the lignin samples were significantly reduced by the A_p stage; in line with other similar works previously
 434 carried out by this research group (Fernández-Rodríguez et al., 2017a). This was also countersigned by the low
 435 presence of sugars in the collected samples, with values between 1.70 and 1.85% except for Tw lignin, in which
 436 the carbohydrate content of the lignin samples was above 2.5%. This increase can be related to the recalcitrance
 437 caused by the LCC formed during the thermal treatment, which were not leached during weathering neither
 438 hydrolyzed during the A_p treatment. This tendency was also observed in alkali lignins from the first bleaching
 439 step (L2), in which both weathered samples (Pw and Tw) presented higher carbohydrate content than their
 440 original counterparts, following the same trend already reported in previous work (Fernández-Rodríguez et al.,
 441 2017b). In any case, the purity of the L2 samples was above 90% (except in the case of Po), demonstrating once
 442 again that the inclusion of a lignin isolation step could be implemented even during the first bleaching stage
 443 since the purity of the lignin was not compromised. Nevertheless, the lignin precipitation from the 2O₂ stage was

444 not justified due to the low amount obtained, which was not big enough to obtain the necessary material even
 445 to conduct its full characterization.
 446 Figure S2 shows a graphical display to explain better the occurring tendencies regarding molecular weight and
 447 polydispersity index. In the untreated pinewood, the molecular weight of lignins after weathering was higher in
 448 all cases (L1, L2, and L3), presenting an almost linear trend and, therefore, a correlation between the Mw of
 449 each lignin type. The Mw of organosolv lignin (L1) in all samples was decreasing after thermal treatment, as it is
 450 represented in Figure S3. On the contrary, the Mw of alkali lignin (L2) increased after the thermal treatment of
 451 the samples.

452
 453 **Table 2.** Composition of the lignin samples collected along the different stages of the experimental procedure.

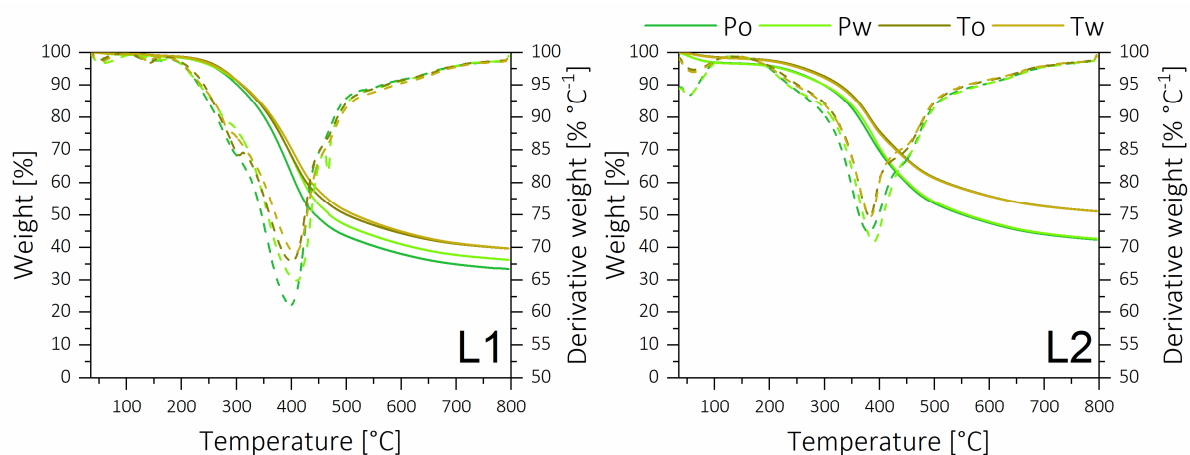
		AIL [%]	ASL [%]	Carbohydrates [%]	Ashes [%]	Mw [g mol ⁻¹]	Mw Mn ⁻¹
Po	L1	93.4	0.88	1.84	1.13	5534	4.43
	L2	83.3	1.46	3.01	1.15	2772	2.94
	L3	-	-	-	-	21,936	12.4
Pw	L1	93.9	0.53	1.83	0.29	7401	5.32
	L2	93.1	1.20	4.44	0.65	10,049	8.68
	L3	-	-	-	-	28,573	9.27
To	L1	93.4	0.74	1.73	0.51	1453	2.36
	L2	92.8	1.08	5.27	1.06	3477	4.16
	L3	-	-	-	-	23,380	12.8
Tw	L1	94.6	0.95	2.58	0.25	4307	3.71
	L2	89.9	1.29	6.11	0.49	3465	3.88
	L3	-	-	-	-	19,233	10.3

454
 455 All the lignin samples (L1, L2, and L3) were subjected to infrared analysis and carbohydrate products. Besides
 456 having different yields depending on the stage from which they were recovered, there were noticeable
 457 differences between the three of them according to their functional groups, with more differences found
 458 depending on the source. Absorption band associated with -OH stretching vibrations of aromatic and aliphatic
 459 groups between 3700 and 2900 cm⁻¹ presented a distinct difference for L1. On the other hand, for L2, the
 460 intensity of that absorbance band was lower in the case of To and Tw compared to Po and Pw, and in the case of
 461 L3, the presence of the OH band was almost imperceptible. The bands between 2900 and 2750 cm⁻¹, which
 462 correspond to CH stretching in -CH₂ and -CH₃, were more intense in the case of bleaching-stage lignins (L2 and
 463 L3) than in Organosolv lignin (L1). Moreover, in L1, the C-H band was more acute for To and Tw, which
 464 correlated with the absence of such bands in H1. This phenomenon can be related to the formation of LCC
 465 during hydrothermal treatment. The band at 1710 cm⁻¹, identified with non-conjugated carboxylic acids, was
 466 present in all lignins, with a tendency to decrease after each treatment (L1>L2>L3). Another particularity was the
 467 increase of the intensity of this band for To and Tw in the case of L1, which can be related to the degradation of
 468 small carbohydrate sugars into carboxylic acids. The band between 1700 and 1400 cm⁻¹ was related to the
 469 aromatic skeletal vibrations of lignin. In this region, the same decreasing tendency can be observed, which
 470 implies a lower quality of lignin found during the cascading recovery. In this region can be highlighted the band
 471 at 1595 and 1510 cm⁻¹, which corresponds to C=C linkages of the skeletal aromatic ring, the band at 1460 cm⁻¹
 472 corresponding to C-H deformation, and the band at 1420 cm⁻¹ corresponding to C-H aromatic ring vibrations. In
 473 the region between 1500 and 1000 cm⁻¹, the prominent guaiacyl lignin bands can be identified, namely 1270,
 474 1120, and 1030 cm⁻¹, which are related to ν (C-O stretching) of the guaiacyl ring, ν (C-H stretching) of the guaiacyl
 475 unit, and ν (C-O and C-H) in-plane deformation of G-type lignin respectively (Derkacheva and Sukhov, 2008;
 476 Fernández-Rodríguez et al., 2017b; Ibarra et al., 2007; Lu et al., 2017; Xu et al., 2013). These bands presented a
 477 gradual decrease after each treatment, with the first alkali extracted lignin (L2) from hydrothermally treated
 478 wood (To and Tw) having the weakest absorbance intensity in this region.



479
480 **Figure 8.** Infrared absorbance spectrograms of the obtained lignins.
481

482 The thermal properties of the different lignin samples were subjected to a thermogravimetric (TG) analysis.
483 Figure 9 presents the thermograms of L1 and L2 lignins under an inert atmosphere; insets show the derivative
484 thermogram. Other parameters, such as the temperatures of 5% mass loss, 50% mass loss, and residues after
485 800 °C, are represented in Figure S4. Regarding the amount of the remaining residue, the main difference was
486 appreciable between the final residue for L2 compared to L1, as L2 residues are between 42.39% (Po) and
487 51.09% (To), while L1 residues are between 33.36 (Po) and 39.74 (Tw). This situation was related to the origin of
488 the lignin since more condensed structures were expected from the 1O₂ stage against L1 from O_T. Besides, it can
489 be highlighted that there was a clear tendency to increase the residue at 800 °C for thermally treated wood,
490 regardless the stage the lignin samples were isolated (L1 or L2). This can be based on the more stable lignin is
491 conformed during the thermal treatment, as it was commented before. The TG analysis under inert atmosphere
492 gives information regarding the potential char production for each lignin; therefore, a higher residue was related
493 to a higher char content. The differences in decay temperatures and the thermal stability of lignins are related to
494 their structure, molecular weight, origin, and the extraction and precipitation methods followed to obtain the
495 lignins (Gordobil et al., 2016). In this sense, L1 presented higher thermal resistance, presenting the maximum
496 degradation temperature at higher temperatures than those of L2. It can also be seen that To and Tw had higher
497 thermal resistance than Po and Pw. Moreover, Pw and Tw had higher maximum degradation temperatures than
498 Po and To, respectively. On the other hand, L2 lignins presented lower differences between Po and To, being Pw,
499 the one with the highest thermal maximum degradation temperature (389 °C), lower than all of the L1 lignins.
500 From the TG analysis, it can be concluded that L2 lignins were more prone to produce char than L1 samples. This
501 can be due to the O_T stage being more effective in extracting less altered lignin structures. Simultaneously, the
502 oxidizing effect of oxygen, hydrogen peroxide, and the alkaline media influence the denaturalization of these
503 compounds, resulting in lignins with more condensed structures.



504
 505 **Figure 9.** Thermograms and derivative weight loss as a function of the temperature of L1 and L2 of the different
 506 samples.

507 To conclude the lignin characterization, the structural composition of the lignin samples was analyzed by the Py-
 508 GC/MS technique. The analysis is carried out based on the work developed by Chen and collaborators (L. Chen et
 509 al., 2015). The identified phenolic derivatives were classified into five categories, namely benzene (B), phenol (P),
 510 catechol (C), guaiacol (G), and syringol (S) derived units. As it is not clear that catechol could be originated from
 511 G or S structures, the results were also expressed as the S/G ratio to facilitate the interpretation of the results.
 512 Guaiacol was the main compound identified by this technique, a typical fact in lignin samples obtained from
 513 softwood species. Thus, the S/G ratio was always close to zero. The highest values were obtained by Po lignin
 514 samples regardless of the stage they were isolated from (L1 and L2). This indicates that both the thermal
 515 treatment and the weathering attack to a more prominent degree the S units, since the natural weathering of
 516 wood (especially UV radiation) and thermal treatment could promote demethoxylation reactions that resulted in
 517 the transformation of S derived units into C and G derived moieties. This tendency has already been reported
 518 (Ma et al., 2016). The G units lead to creating more condensed structures due to their availability of the C5 in the
 519 aromatic ring. Lignin samples from To feedstock show the second highest values; thus, weathering causes this
 520 degradation mechanism to a higher degree than the thermal treatment. Among samples from different stages,
 521 the differences were not significant, although there was a trend to reduce the S/G in L2 samples in comparison
 522 with L1, a fact that can be explained for the mechanisms described before since, during the 102 stage, more
 523 demethoxylation reactions of the S units could appear. Moreover, they followed a similar decreasing tendency in
 524 both organosolv and alkaline lignins after the weathering treatment.

525
 526 **Table 3.** The abundance of the different phenolic-derived units in the lignins respects the total phenolic moieties
 527 detected.

		Benzene	Phenol	Catechol	Guaiacol	Syringol	S/G ratio
L1	Po	0.26	3.47	2.67	81.4	12.2	0.15
	Pw	0.10	5.49	8.71	83.9	1.82	0.02
	To	0.00	4.14	9.34	76.1	10.4	0.14
	Tw	0.00	7.01	10.1	82.9	0.00	0.00
L2	Po	0.21	3.40	5.97	80.2	10.3	0.13
	Pw	0.27	4.41	5.8	87.2	2.37	0.03
	To	0.20	4.02	8.32	83.8	3.69	0.04
	Tw	0.00	3.51	6.60	89.0	0.93	0.01

528
 529
 530 **Conclusions**

531 The present work proposed a cascade valorization of thermally treated wood after service-life by fractioning its
532 macromolecular components through green processes. To assess the quality of the obtained materials, they
533 were compared with untreated wood and unweathered counterparts. Results showed that the macromolecular
534 constituent that presented the most stability regardless of the conditions was cellulose, having little structural
535 properties changes regardless of the feedstock used as raw material, which demonstrated the robustness of the
536 designed process as the main product in yield was very homogeneous, a fact that would enable the scalability of
537 this global process. The extracted hemicelluloses consisted of high purity mannose oligomers; however, due to
538 the difficulties of precipitating hemicelluloses in its polymer nature, the use of the organosolv process and the
539 acid leaching were not enough to justify a valorization of hemicelluloses, as their low extraction yields
540 demonstrated it. Lignins were the macromolecules presenting more variations, with significant differences
541 depending on the extraction phase (organosolv pulping or oxygen-alkali bleaching) and the material source. With
542 thermally treated wood having more LCC (oxygen-alkali lignin) but also the best yield of AIL (organosolv lignin),
543 however, in general, the purity and the thermal stability of all the lignins resulted in high values for either lignin,
544 stating that the selected processes are robust and appropriate for the fractioning of pinewood after being
545 thermally treated and weathered.

546 **Supporting Information.**

547 Please consult the supplementary information for additional data.

548 **Acknowledgments**

549 The authors would like to acknowledge the University of the Basque Country UPV/EHU for financially supporting
550 this work. E.R. wants to acknowledge the tenure track position "Bois: Biobased materials" part of E2S UPPA
551 supported by the "Investissements d'Avenir" French program managed by ANR (ANR-16-IDEX-0002). R.H. wants
552 to acknowledge the Basque Government for financial support through the INGVTCL4-D00112-7 contract and
553 European Commission for funding the InnoRenew project (Grant Agreement # 739574) under the Horizon2020
554 Widespread-Teaming program, the Republic of Slovenia (investment funding from the Republic of Slovenia and
555 the European Union European Regional Development Fund), and infrastructural ARRS program IO-0035. The
556 authors thank for technical and human support provided by SGiker of UPV/EHU for XRD characterizations.

557 **References**

- 558 Barana, D., Salanti, A., Orlandi, M., Ali, D.S., Zoia, L., 2016. Biorefinery process for the simultaneous recovery of
559 lignin, hemicelluloses, cellulose nanocrystals and silica from rice husk and *Arundo donax*. *Ind. Crops Prod.*
560 86, 31–39. <https://doi.org/10.1016/j.indcrop.2016.03.029>
- 561 Bentsen, N.S., Felby, C., 2012. Biomass for energy in the European Union - A review of bioenergy resource
562 assessments. *Biotechnol. Biofuels.* <https://doi.org/10.1186/1754-6834-5-25>
- 563 Boonstra, M.J., Tjeerdsma, B., 2006. Chemical analysis of heat treated softwoods.
564 <https://doi.org/10.1007/s00107-005-0078-4>
- 565 Bruno M. Esteves, René Herrera, Jorge Santos, Luísa Carvalho, Lina Nunes, José Ferreira, Idalina J. Domingos,
566 Luísa Cruz-Lopes, 2020. Artificial weathering of heat-treated pines from the Iberian peninsula ::
567 *BioResources. Bioresources* 15, 9642–9655.
- 568 Campbell-Johnston, K., Vermeulen, W.J.V., Reike, D., Bullot, S., 2020. The circular economy and cascading:
569 towards a framework. *Resour. Conserv. Recycl. X* 100038. <https://doi.org/10.1016/J.RCRX.2020.100038>
- 570 Cantero, A., 2014. El futuro del pino radiata en el País Vasco. *Sustrai* 52–55.
- 571 Chen, L., Wang, X., Yang, H., Lu, Q., Li, D., Yang, Q., Chen, H., 2015. Study on pyrolysis behaviors of non-woody
572 lignins with TG-FTIR and Py-GC/MS. *J. Anal. Appl. Pyrolysis* 113, 499–507.
573 <https://doi.org/10.1016/J.JAAP.2015.03.018>
- 574 Chen, Z., Hu, T.Q., Jang, H.F., Grant, E., 2015. Modification of xylan in alkaline treated bleached hardwood kraft
575 pulps as classified by attenuated total-internal-reflection (ATR) FTIR spectroscopy. *Carbohydr. Polym.* 127,
576 418–426. <https://doi.org/10.1016/J.CARBPOL.2015.03.084>
- 577 da Silva, C.M.S., Vital, B.R., Rodrigues, F. de Á., de Almeida, Ê.W., Carneiro, A. de C.O., Cândido, W.L., 2019.
578 Hydrothermal and organic-chemical treatments of eucalyptus biomass for industrial purposes. *Bioresour.*
579 *Technol.* 289, 121731. <https://doi.org/10.1016/j.biortech.2019.121731>
- 580 Dammer, L., Bowyer, C., Breitmayer, E., Eder, A., Nanni, S., Allen, B., Carus, M., Essel, R., 2016. Cascading Use of
581 Wood Products. Gland, Switzerland.

582 de Hoyos-Martínez, P.L., Erdocia, X., Charrier-El Bouhtoury, F., Prado, R., Labidi, J., 2018. Multistage treatment of
583 almonds waste biomass: Characterization and assessment of the potential applications of raw material and
584 products. *Waste Manag.* 80, 40–50. <https://doi.org/10.1016/J.WASMAN.2018.08.051>
585 Derkacheva, O., Sukhov, D., 2008. Investigation of Lignins by FTIR Spectroscopy. *Macromol. Symp.* 265, 61–68.
586 <https://doi.org/10.1002/masy.200850507>
587 Durmaz, E., Ucuncu, T., Karamanoglu, M., Kaymakci, A., n.d. Effects of Heat Treatment on Some Characteristics
588 of Scots Pine (*Pinus sylvestris* L.) Wood.
589 Etxabe Villasante, J., 2018. The Potential of Wood-Based Bioenergy in the Basque Country. University of Twente,
590 Twente.
591 European Committee for Standardization, 2008. Thermal modified timber - Definitions and characteristics.
592 Technical specification no. CEN/TS 15679:2008. Brussels.
593 Fernández-Rodríguez, J., Erdocia, X., Hernández-Ramos, F., Gordobil, O., González Alriols, M., Labidi, J., 2020.
594 Direct lignin depolymerization process from sulfur-free black liquors. *Fuel Process. Technol.* 197, 106201.
595 <https://doi.org/10.1016/j.fuproc.2019.106201>
596 Fernández-Rodríguez, J., Erdocia, X., Sánchez, C., Alriols, M.G., Labidi, J., 2017a. Lignin depolymerization for
597 phenolic monomers production by sustainable processes. *J. Energy Chem.* 26, 622–631.
598 <https://doi.org/10.1016/j.jechem.2017.02.007>
599 Fernández-Rodríguez, J., Gordobil, O., Robles, E., González-Alriols, M., Labidi, J., 2017b. Lignin valorization from
600 side-streams produced during agricultural waste pulping and total chlorine free bleaching. *J. Clean. Prod.*
601 142, 2609–2617. <https://doi.org/10.1016/j.jclepro.2016.10.198>
602 George, B., Suttie, E., Merlin, A., Deglise, X., 2005. Photodegradation and photostabilisation of wood – the state
603 of the art. *Polym. Degrad. Stab.* 88, 268–274. <https://doi.org/10.1016/J.POLYMDEGRADSTAB.2004.10.018>
604 Gordobil, O., Moriana, R., Zhang, L., Labidi, J., Sevastyanova, O., 2016. Assesment of technical lignins for uses in
605 biofuels and biomaterials: Structure-related properties, proximate analysis and chemical modification. *Ind.*
606 *Crops Prod.* 83, 155–165. <https://doi.org/10.1016/j.indcrop.2015.12.048>
607 Gullón, P., Gullón, B., Astray, G., Carpena, M., Fraga-Corral, M., Prieto, M.A., Simal-Gandara, J., 2020. Valorization
608 of by-products from olive oil industry and added-value applications for innovative functional foods. *Food*
609 *Res. Int.* <https://doi.org/10.1016/j.foodres.2020.109683>
610 Herrera-Díaz, R., Sepúlveda-Villarreal, V., Torres-Mella, J., Salvo-Sepúlveda, L., Llano-Ponte, R., Salinas-Lira, C.,
611 Peredo, M.A., Ananías, R.A., 2019. Influence of the wood quality and treatment temperature on the
612 physical and mechanical properties of thermally modified radiata pine. *Eur. J. Wood Wood Prod.* 77, 661–
613 671. <https://doi.org/10.1007/s00107-019-01424-9>
614 Herrera, R., Arrese, A., de Hoyos-Martínez, P.L., Labidi, J., Llano-Ponte, R., 2018. Evolution of thermally modified
615 wood properties exposed to natural and artificial weathering and its potential as an element for façades
616 systems. *Constr. Build. Mater.* 172, 233–242. <https://doi.org/10.1016/J.CONBUILDMAT.2018.03.157>
617 Herrera, R., da Silva, D.T., Llano-Ponte, R., Labidi, J., 2016a. Characterization of pine wood liquid and solid
618 residues generated during industrial hydrothermal treatment. *Biomass and Bioenergy* 95, 174–181.
619 <https://doi.org/10.1016/j.biombioe.2016.10.006>
620 Herrera, R., Erdocia, X., Llano-Ponte, R., Labidi, J., 2014. Characterization of hydrothermally treated wood in
621 relation to changes on its chemical composition and physical properties. *J. Anal. Appl. Pyrolysis* 107, 256–
622 266. <https://doi.org/10.1016/j.jaap.2014.03.010>
623 Herrera, R., Krystofiak, T., Labidi, J., Llano-Ponte, R., 2016b. Characterization of Thermally Modified Wood at
624 Different Industrial Conditions. *Drewno* 59. <https://doi.org/10.12841/wood.1644-3985.CO5.15>
625 Hosseinaei, O., Harper, D.P., Bozell, J.J., Rials, T.G., 2016. Role of Physicochemical Structure of Organosolv
626 Hardwood and Herbaceous Lignins on Carbon Fiber Performance. *ACS Sustain. Chem. Eng.* 4, 5785–5798.
627 <https://doi.org/10.1021/acssuschemeng.6b01828>
628 Ibarra, D., Camarero, S., Romero, J., Martínez, M.J., Martínez, A.T., 2006. Integrating laccase–mediator treatment
629 into an industrial-type sequence for totally chlorine-free bleaching of eucalypt kraft pulp. *J. Chem. Technol.*
630 *Biotechnol.* 81, 1159–1165. <https://doi.org/10.1002/jctb.1485>
631 Ibarra, D., Chávez, M.I., Rencoret, J., del Río, J.C., Gutiérrez, A., Romero, J., Camarero, S., Martínez, M.J., Jiménez-
632 Barbero, J., Martínez, Á.T., 2007. Structural modification of eucalypt pulp lignin in a totally chlorine-free
633 bleaching sequence including a laccase-mediator stage. *Holzforschung* 61, 634–646.
634 <https://doi.org/10.1515/HF.2007.096>
635 Islam, M.K., Wang, H., Rehman, S., Dong, C., Hsu, H.Y., Lin, C.S.K., Leu, S.Y., 2020. Sustainability metrics of
636 pretreatment processes in a waste derived lignocellulosic biomass biorefinery. *Bioresour. Technol.*
637 <https://doi.org/10.1016/j.biortech.2019.122558>
638 Jones, D., Sandberg, D., 2020. View of A Review of Wood Modification Globally – Updated Findings from COST
639 FP1407 | Interdisciplinary Perspectives on the Built Environment. *Interdiscip. Perspect. Built Environ.* 1, 1–
640 31. <https://doi.org/10.37947/ipbe.2020.vol1.1>

641 Keegan, D., Kretschmer, B., Elbersen, B., Panoutsou, C., 2013. Cascading use: a systematic approach to biomass
642 beyond the energy sector. *Biofuels, Bioprod. Biorefining* 7, 193–206. <https://doi.org/10.1002/bbb.1351>

643 Kong, F., Ni, Y., He, Z., 2009. A partial magnesium hydroxide substitution for sodium hydroxide in peroxide
644 bleaching of an aspen CTMP. *J. Wood Chem. Technol.* 29, 136–149.
645 <https://doi.org/10.1080/02773810902822355>

646 Kodynska, D., 2011. Chelating Agents of a New Generation as an Alternative to Conventional Chelators for
647 Heavy Metal Ions Removal from Different Waste Waters, in: *Expanding Issues in Desalination*. InTech.
648 <https://doi.org/10.5772/21180>

649 Krueger-Zerhusen, N., Cantero-Tubilla, B., Wilson, D.B., 2018. Characterization of cellulose crystallinity after
650 enzymatic treatment using Fourier transform infrared spectroscopy (FTIR). *Cellulose* 25, 37–48.
651 <https://doi.org/10.1007/s10570-017-1542-0>

652 Li, T., Cheng, D. li, Avramidis, S., Wälinder, M.E.P., Zhou, D. guo, 2017. Response of hygroscopicity to heat
653 treatment and its relation to durability of thermally modified wood. *Constr. Build. Mater.* 144, 671–676.
654 <https://doi.org/10.1016/j.conbuildmat.2017.03.218>

655 Lu, Y., Lu, Y.-C., Hu, H.-Q., Xie, F.-J., Wei, X.-Y., Fan, X., 2017. Structural Characterization of Lignin and Its
656 Degradation Products with Spectroscopic Methods. *J. Spectrosc.* 2017, 1–15.
657 <https://doi.org/10.1155/2017/8951658>

658 Ma, Z., Sun, Q., Ye, J., Yao, Q., Zhao, C., 2016. Study on the thermal degradation behaviors and kinetics of alkali
659 lignin for production of phenolic-rich bio-oil using TGA–FTIR and Py–GC/MS. *J. Anal. Appl. Pyrolysis* 117,
660 116–124. <https://doi.org/10.1016/J.JAAP.2015.12.007>

661 Maskal, J., Thompson, I.M., 1971. Magnesium hydroxide-containing paper. US3941610A.

662 Nelson, P.J., 1998. Elemental chlorine free (ECF) and totally chlorine free (TCF) bleaching of pulps, in: Young, R.A.
663 (Ed.), *Environmentally Friendly Technologies for the Pulp and Paper Industry*. John Wiley & Sons, Inc., San
664 Francisco, CA.

665 Ni, Y., He, Z., 2004. Review: Using magnesium hydroxide as the alkali source for peroxide bleaching of
666 mechanical pulps-process chemistry and industrial implementation, Hu et al. Xu.

667 Nitsos, C., Rova, U., Christakopoulos, P., 2018. Organosolv fractionation of softwood biomass for biofuel and
668 biorefinery applications. *Energies* 11. <https://doi.org/10.3390/en11010050>

669 Oliaei, E., Lindén, P.A., Wu, Q., Berthold, F., Berglund, L., Lindström, T., 2020. Microfibrillated lignocellulose
670 (MFLC) and nanopaper films from unbleached kraft softwood pulp. *Cellulose* 27, 2325–2341.
671 <https://doi.org/10.1007/s10570-019-02934-8>

672 Olsson, O., Bruce, L., Hektor, B., Roos, A., Guisson, R., Lamers, P., Hartley, D., Ponitka, J., Hildebrand, D., Thrän,
673 D., 2016. Cascading of woody biomass: definitions, policies and effects on international trade.

674 Pandey, M.P., Kim, C.S., 2011. Lignin Depolymerization and Conversion: A Review of Thermochemical Methods.
675 *Chem. Eng. Technol.* 34, 29–41. <https://doi.org/10.1002/ceat.201000270>

676 Peng, F., Peng, P., Xu, F., Sun, R.C., 2012. Fractional purification and bioconversion of hemicelluloses. *Biotechnol.*
677 *Adv.* 30, 879–903. <https://doi.org/10.1016/j.biotechadv.2012.01.018>

678 Pettersen, R., 1984. The Chemistry of Solid Wood, in: Rowell, R.M. (Ed.), *The Chemistry of Solid Wood*. American
679 Chemical Society, Washington, D.C., pp. 1–9. <https://doi.org/10.1021/ba-1984-0207>

680 Pinto, I.S.S., Ascenso, O.S., Barros, M.T., Soares, H.M.V.M., 2015. Pre-treatment of the paper pulp in the
681 bleaching process using biodegradable chelating agents. *Int. J. Environ. Sci. Technol.* 12, 975–982.
682 <https://doi.org/10.1007/s13762-013-0480-0>

683 Reyes, P., Mendonça, R.T., Aguayo, M.G., Rodríguez, J., Vega, B., Fardim, P., 2013. Extraction and
684 characterization of hemicelluloses from *Pinus radiata* and its feasibility for bioethanol production. *Rev.*
685 *Árvore* 37, 175–180. <https://doi.org/10.1590/S0100-67622013000100018>

686 Robles, E., Fernández-Rodríguez, J., Barbosa, A.M., Gordobil, O., Carreño, N.L.V., Labidi, J., 2018. Production of
687 cellulose nanoparticles from blue agave waste treated with environmentally friendly processes. *Carbohydr.*
688 *Polym.* 183, 294–302. <https://doi.org/10.1016/j.carbpol.2018.01.015>

689 Sandberg, D., Kutnar, A., 2016. Thermal Modified Timber (Tmt): Recent Development in Europe and North
690 America. *Wood Fiber Sci.* 48, 28–39.

691 Santos, T.M., Alonso, M.V., Oliet, M., Domínguez, J.C., Rigual, V., Rodríguez, F., 2018. Effect of autohydrolysis on
692 *Pinus radiata* wood for hemicellulose extraction. *Carbohydr. Polym.* 194, 285–293.
693 <https://doi.org/10.1016/j.carbpol.2018.04.010>

694 Sokka, L., Koponen, K., Keränen, J.T., 2015. Cascading use of wood in Finland-with comparison to selected EU
695 countries. *Espoo*.

696 Sun, X.-F., Wang, H., Jing, Z., Mohanathas, R., 2013. Hemicellulose-based pH-sensitive and biodegradable
697 hydrogel for controlled drug delivery. *Carbohydr. Polym.* 92, 1357–1366.
698 <https://doi.org/10.1016/J.CARBPOL.2012.10.032>

699 TAPPI T 204 cm-07, 2007. Solvent extractives of wood and pulp. Peachtree Corners, GA.

700 TAPPI T 211 om-16, 2016. Ash in wood, pulp, paper and paperboard: combustion at 525 degrees. Peachtree
701 Corners, GA.

702 TAPPI T 222 om-11, 2011. Acid-insoluble lignin in wood and pulp. Peachtree Corners, GA.

703 TAPPI T 249 cm-09, 2009. Carbohydrate composition of extractive-free wood and wood pulp by gas-liquid
704 chromatography. Peachtree Corners, GA.

705 TAPPI T 264 cm-07, 2007. Preparation of Wood for Chemical Analysis, Standard by Technical Association of the
706 Pulp and Paper Industry. Atlanta, GA.

707 Toledano, A., Serrano, L., Balu, A.M., Luque, R., Pineda, A., Labidi, J., 2013. Fractionation of Organosolv Lignin
708 from Olive Tree Clippings and its Valorization to Simple Phenolic Compounds. *ChemSusChem* 6, 529–536.
709 <https://doi.org/10.1002/cssc.201200755>

710 Wang, S., Zhou, Y., Liang, T., Guo, X., 2013. Catalytic pyrolysis of mannose as a model compound of hemicellulose
711 over zeolites. *Biomass and Bioenergy* 57, 106–112. <https://doi.org/10.1016/J.BIOMBIOE.2013.08.003>

712 Wei, J., Rao, F., Huang, Y., Zhang, Y., Qi, Y., Yu, W., Hse, C.Y., 2019. Structure, mechanical performance, and
713 dimensional stability of radiata pine (*Pinus radiata* D. Don) scrimbers. *Adv. Polym. Technol.* 2019.
714 <https://doi.org/10.1155/2019/5209624>

715 Wise, L.E., Murphy, M., D’Addieco, A.A., 1946. Chlorite holocellulose, its fractionation and bearing on summative
716 wood analysis and on studies on the hemicelluloses. *Pap. Trade J.* 122, 35–43.

717 Xu, F., Yu, J., Tesso, T., Dowell, F., Wang, D., 2013. Qualitative and quantitative analysis of lignocellulosic biomass
718 using infrared techniques : A mini-review. *Appl. Energy* 104, 801–809.
719 <https://doi.org/10.1016/j.apenergy.2012.12.019>

720 Yildiz, S., Gümüşkaya, E., 2007. The effects of thermal modification on crystalline structure of cellulose in soft
721 and hardwood. *Build. Environ.* 42, 62–67. <https://doi.org/10.1016/j.buildenv.2005.07.009>

722 Zakzeski, J., Bruijninx, P.C.A., Jongorius, A.L., Weckhuysen, B.M., 2010. The Catalytic Valorization of Lignin for
723 the Production of Renewable Chemicals. *Chem. Rev.* 110, 3552–3599. <https://doi.org/10.1021/cr900354u>

724 Zhao, X., Li, S., Wu, R., Liu, D., 2017. Organosolv fractionating pre-treatment of lignocellulosic biomass for
725 efficient enzymatic saccharification: chemistry, kinetics, and substrate structures. *Biofuels, Bioprod.*
726 *Biorefining* 11, 567–590. <https://doi.org/10.1002/bbb.1768>

727